

## MPPT ALGORITHM USING DECREMENTED WINDOW-SCANNING METHOD FOR HOME SCALE PHOTOVOLTAIC-BASED POWER SUPPLY SYSTEMS

FAIZAL ARYA SAMMAN<sup>1,\*</sup>, TINO SUHAEBRI<sup>2</sup>, RHIZA SAMSOE' OED SADJAD<sup>1</sup>  
ANDI EJAH UMRAENI SALAM<sup>1</sup>, ANDANI ACHMAD<sup>1</sup> AND CARMADI MACHBUB<sup>3</sup>

<sup>1</sup>Department of Electrical Engineering  
Universitas Hasanuddin

Jl. Poros Malino Km. 6, Bontomarannu 92171, South Sulawesi, Indonesia

\*Corresponding author: faizalas@unhas.ac.id

<sup>2</sup>Department of Electrical and Installation Engineering

Akademi Komunitas Industri Manufaktur Bantaeng

Pa'jukukang, Nipa-Nipa, Bantaeng 92461, South Sulawesi, Indonesia

<sup>3</sup>School of Electrical Engineering and Informatics

Institut Teknologi Bandung (ITB)

Jl. Ganesha No. 10, Bandung 40132, West Java, Indonesia

Received June 2020; revised December 2020

**ABSTRACT.** *This paper presents a hardware implementation of a novel method to operate a photovoltaic-based electric power system at its maximum power point. A maximum power point tracing (MPPT) algorithm named decremented window-scanning (DWS) is proposed and validated in real experiments. The scanning process operates based on perturbing signal with variable duty ratios of the pulse-width modulated signal applied to a DC-DC converter circuit in the MPPT module. The characteristic of the proposed MPPT algorithm is its simplicity to implement on a microcontroller device. It consumes 11,518 bytes memory, or 37% of total 30,720 byte available memory slots in the microcontroller. The MPPT algorithm is tested using 100Wp photovoltaic (PV) panel under three different partial shading conditions. The experimental results show that the MPPT unit can find the expected duty ratios that can turn the PV unit to operate at its maximum power points.*

**Keywords:** Maximum power point tracing (MPPT) algorithm, Power electronics, Scanning-based MPPT algorithm, Photovoltaic systems, Decrement window-scanning

1. **Introduction.** Environment issue is one of main factors to accelerate the optimal uses of renewable energies. Wind energy, fuel cell, photovoltaic and thermoelectric generator are promising technologies that can potentially replace the use of fossil fuel energies. To make use of renewable energies, an appropriate power system generation is required. According to the power generation volume, renewable energy-based (RE-based) power system generation can be classified into large scale, medium scale, small scale and micro scale power system generation. Home scale RE-based power system generation can be classified into the micro scale system. A house locally powered by renewable energies, such as photovoltaic energy, or renown as an energy autonomy house, will be a trending issue in the future.

This paper discusses an issue in home scale renewable energy-based power system generation, which is based on hybrid photovoltaic-grid power supply system. The hybrid system is shown in Figure 1. The system consists of an MPPT module, which is the main

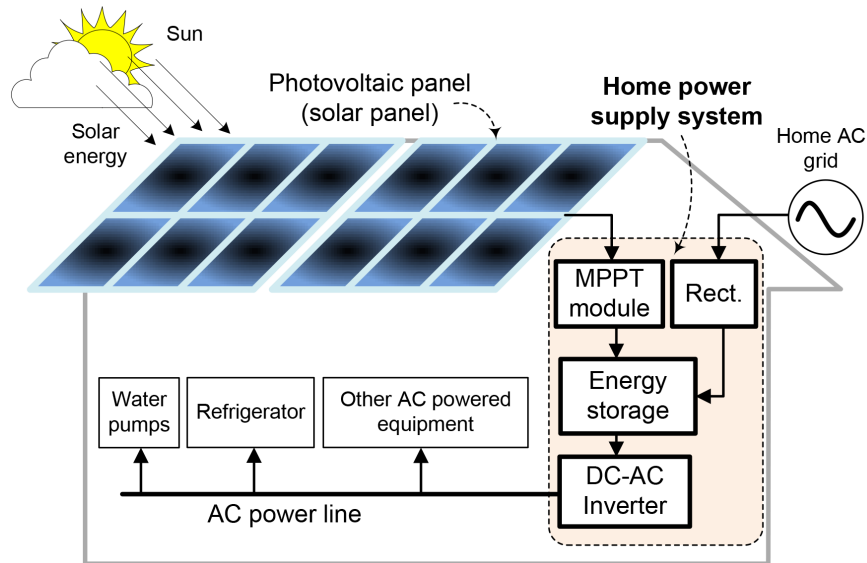


FIGURE 1. A home scale power supply system based on DC coupled photovoltaic-grid

domain discussion of this paper, an energy storage unit, an inverter used to convert DC power to AC power, and a rectifier that converts AC power grid to DC power. The energy storage unit is used to store excessive energy from PV panels and to dispatch energy when renewable energy is not available. Since renewable energy, including solar energy is an ambient energy, a hybrid home scale power supply system should be combined with AC power grid. In the figure, it seems that the DC power from photovoltaic (PV) panels is combined with the AC power grid with DC coupling technique. However, this issue is not discussed further in this paper.

In the hybrid RE-based power supply system described before, there are some important issues to address. One of the important issues in the systems is the continuous operations of the PV system in its maximum power point. This issue must be addressed, because of the characteristic of recently developed solar cell technologies. Figure 2(a) presents a power curve that represents the power characteristic of a PV panel. It is very important that a PV system operates at its maximum power point (MPP). MPP is an operating point, at certain current value ( $I_{mpp}$ ) and voltage value ( $V_{mpp}$ ) in the PV power curve, where maximum power from the PV system is delivered.  $I_{SC}$  is a short circuit current, as the PV operates at a zero voltage point. When the PV operates between the zero voltage point and the maximum voltage value ( $V_{mpp}$ ), the power tends to increase linearly until it reaches its maximum power value ( $P_{mpp}$ ). When a PV module operates between the  $V_{mpp}$  and its open circuit voltage ( $V_{OC}$ ), the output current of the PV panel will drop drastically until it reaches its zero current value. Therefore, although the voltage becomes higher, the output power will drop due to the current drop. The PV does not fully convert the solar energy to be electric energy, but part of them is converted to thermal energy.

In order to maintain a PV system operating at its maximum power point, a maximum power point tracking (MPPT) controller system should be proposed and designed to overcome the problem. An MPPT control algorithm that is designed to keep the PV system working in its maximum power point is commonly called the maximum power point tracking algorithm or MPPT algorithm. There are many techniques to implement the MPPT algorithm. One of the famous methods is named perturb-and-observe (P&O) technique. Using this method, the implemented control unit will perturb the power converter circuit (a boost or a buck-boost converter) with a pulse-width modulated (PWM) signal. The

PWM perturbation is normally started with a pre-determined duty ratio. As the PWM signal is applied, the output power of the PV modules is measured.

Another important issue in the PV operation is partial shading problem. When any parts of the PV surface are covered by materials, or the sunlight direction to any parts of the PV surface is shadowed by certain objects, then the partial shading problem occurs. Figure 2(b) shows power curves of a PV panel in normal condition or when a partial shading takes place. In the partial shading condition, the power curve is normally dropped, including the maximum power point (MPP). When the PV cells are configured with a bypass/blocked diode, a few local maximum power points (LMPPs) appear in the power curve beside the global maximum power point (GMPP). GMPP is the highest maximum power point in the power curve. In this condition, an extra control algorithm in the MPPT unit must be implemented. The control algorithm should be able to find the global MPP. Otherwise, the MPPT unit will operate the PV at the unexpected MPP or be trapped at a local MPP.

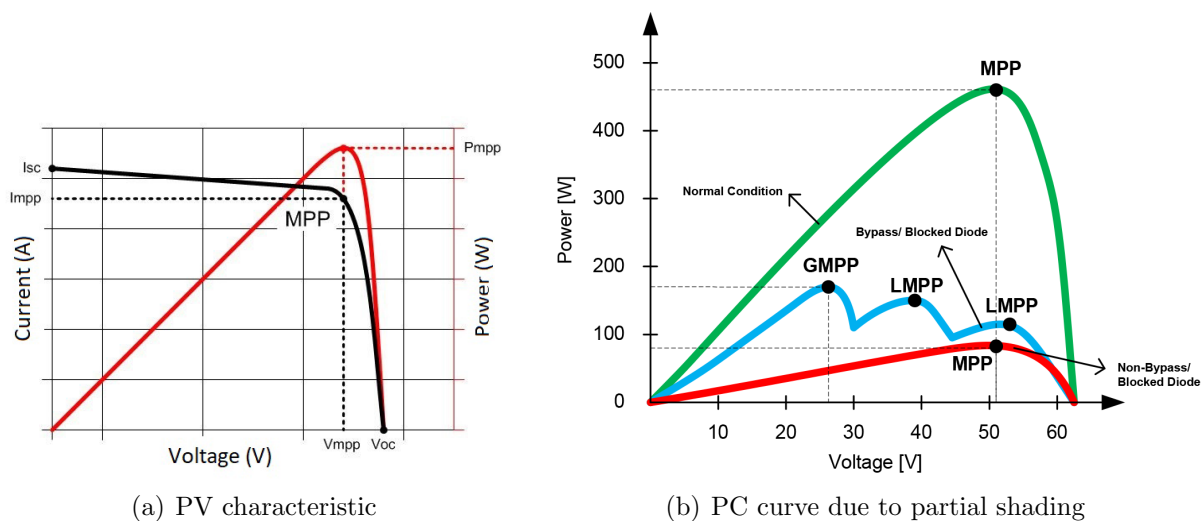


FIGURE 2. PV characteristic without and with partial shading condition

There is some literature that proposes conventional and non-conventional techniques to handle the partial shading problem. Our paper presents a new simple idea to design an MPPT control algorithm and its real hardware implementation to solve the partial shading problem. The implemented MPPT algorithm is named “decremented window-size scanning method” and will be later explained in detail. The rest parts of the paper are discussed in the following section. Section 2 gives some previous works related to our current work. Section 3 discusses the electronic hardware and embedded software implementation of the MPPT system. Section 4 presents the experimental results to test the MPPT module under partial shading conditions. Section 5 summarizes the work and gives brief outlooks.

**2. Related Works and Contribution.** There are many techniques that can be used to operate PV systems in its maximum power point. MPPT algorithms have been implemented using conventional and non-conventional methods such as artificial neural networks (ANNs), fuzzy logic systems, and nature-inspired algorithms such as particle swarm optimization (PSO) methods. Each of the engineering approaches has advantages and disadvantages from specific viewpoints.

Conventional methods can be implemented using for example, incremental conductance [1,2], perturb-and-observe with binary searching [3], and fractional short-circuit current

method [4]. Another conventional MPPT technique is hill climbing method [5]. Conventional methods are simple to implement, but they can suffer from any conditions, where partial shadows are difficult to predict. In any cases, compounding the conventional techniques with other non-conventional can improve the MPPT's performances.

Non-conventional methods are more complex to implement, but they can find optimal solution under highly non-linear power point curves. The work in [6] discusses the use of fuzzy adaptive radial basis function neural network (RBF-NN) to implement the MPPT algorithms. This work combines fuzzy logic, which is used to search for a variable voltage step size that reduces oscillation around an MPP, and an adaptive RBF-NN, which is used to maintain the PV module voltage at its optimal state resulted from the fuzzy logic system. The implementation of fuzzy logic controller (FLC) for the MPPT is also presented in [7,8]. The fuzzy controller can be used to continuously track the non-linear characteristics of PV modules, where its membership functions are optimized using metaheuristic techniques [9]. The FLC can also be combined with a specialized adaptive calculation block to improve the accuracy and the speed of the global MPP searching [10]. The adaptive calculation block is used to generate a reference voltage for each MPP voltage according to any variable atmospheric conditions.

The work in [11] uses Gaussian support vector machine and artificial neural network techniques. The work in [12] uses a standard PSO with perturb-and-observe (P&O) algorithm to harvest maximum energy from PV panels, while the work in [13] uses an improved PSO called grey wolf optimization, and [14] uses simplified accelerated PSO (SAPSO), which combines PSO algorithm and the traditional hill climbing algorithm. The neuro-fuzzy system can also be used to improve the performance of the conventional incremental-conductance (IC) MPPT method [15]. The neuro-fuzzy controller is used to adapt the step size of the incremental conductance MPPT method.

In terms of signal processing method, the MPPT algorithm can be implemented in analog or in digital signal processing. In general, most of MPPT algorithms presented in literature use digital signal processing approach. An MPPT unit with analog signal processing will require less devices or component and has potential to reduce power consumption [16,17]. However, analog techniques are sensitive to noise and parameter drifts of the components used in the analog circuits. Most of MPPT algorithms use digital technique. This technique is favorable due to its flexibility to reconfigure the implemented MPPT algorithms.

An MPPT algorithm in PV system application using partitioned self-adaption variable step size is discussed in [18]. The work in [19] proposes an MPPT algorithm that uses a variable step algorithm to ensure the current control signal. The signal is used to obtain a control actuation based on predicted mean value. Another work that uses scan methods to search for a global MPPT is for example presented in [20]. It periodically inspects the voltage-current of PV panels in real time to detect hotspot PV cells, which is used to determine a partial shading condition. The work uses perturbing voltage ( $\Delta V$ ) of about 0.1V, with sampling interval ( $\Delta t$ ) of 1s. The work in [21] avoids to use a blind global scan techniques, by determining the appearance of partial shading and computing the number of local MPPs. Similar to the previous work, it scans also using perturbing voltage  $\Delta V$ .

The complexity of the non-conventional methods can give negative impact to power consumption of the computing algorithms. ANN-based approach for example requires large collective data to train the corresponding ANN. Therefore, any situations that are not represented by the training data could degrade the system performance, and a new training process is then required. However, in some cases, the ANN-based techniques can outperform the conventional techniques.

Our work presents a new MPPT algorithm called decremented window-size (DWS) scanning. The DWS scanning-based MPPT method is implementable on a microcontroller unit with relatively low computing complexity. Compared to non-conventional techniques, which use, e.g., artificial neural network, fuzzy logic systems and/or bio/nature-inspired algorithms, the DWS scanning method is classified into a conventional technique, which is simple to implement. A prior knowledge and information about PV characteristics, which is used to train the system like in non-conventional techniques, is not required. Therefore, once the MPPT module gets started, the algorithm will directly work to search for a global MPP without the offline pre-computation training program.

Compared to some of the aforementioned works that use perturbing voltage, our proposed DWS scanning method uses perturbing duty cycle ( $\Delta D$ ) to observe the power points. The perturbing duty cycle is easier to implement in a microcontroller unit, since this parameter is directly tuned in the corresponding computer program. Compared to a few works as mentioned before, our MPPT module does not use an adaptive or variable step size in the scanning process. The adaptive technique can improve the MPPT performance, but it makes the computer program more complex and consumes more computing power and energy.

**3. Hardware and Software Design.** There are two main parts of the designed MPPT module, i.e., a hardware module and an embedded software. The hardware is realized in a printed circuit board (PCB), where a microcontroller is mounted on the PCB. The software is embedded in the microcontroller, which is a soft implementation of the decremented window-scanning (DWS) MPPT algorithm. Both main parts are described in the following subsections.

**3.1. The MPPT system diagram.** Figure 3 shows the proposed block diagram of an MPPT unit that will be discussed in this paper. A single-ended primary inductive converter (SEPIC) circuit is used as a power circuit bridge to deliver power from the PV panel to the system load. The MPPT algorithm, embedded on a microcontroller, generates a pulse-width modulated (PWM) signal with variable duty ratio, that is used

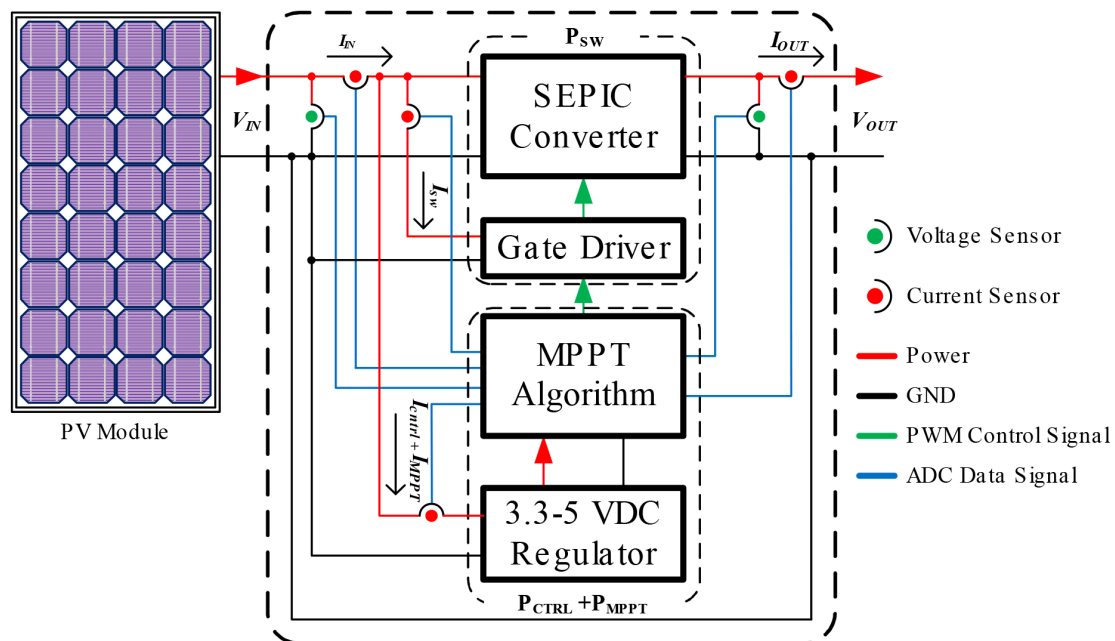


FIGURE 3. The block diagram of the proposed MPPT unit

to control the SEPIC circuit through a MOSFET's gate driver. The MPPT is energized from the PV power through a 3.3-5V DC voltage regulator. The MPPT measures PV's output power and SEPIC's output power by sensing the voltage and current from both output terminals. It measures also electric current flowing to the gate driver. The current measurement is used to analyze the power consumption of the MPPT module.

**3.2. The MPPT hardware module.** The hardware module consists of two main boards, i.e., a microcontroller unit (MCU) board and a power electronic board, named also as the MPPT circuit board. On the power electronic board, there are a DC-DC power converter circuit, sensor circuits, and other electronic parts such as voltage regulator, passive components, fuse, and heat sink. The hardware photograph of the power electronic board is presented in Figure 4(a). On the MCU board, there is a microcontroller, in which an MPPT control algorithm is embedded. The explanation about the soft implementation of the algorithm will be presented in Section 3.3.

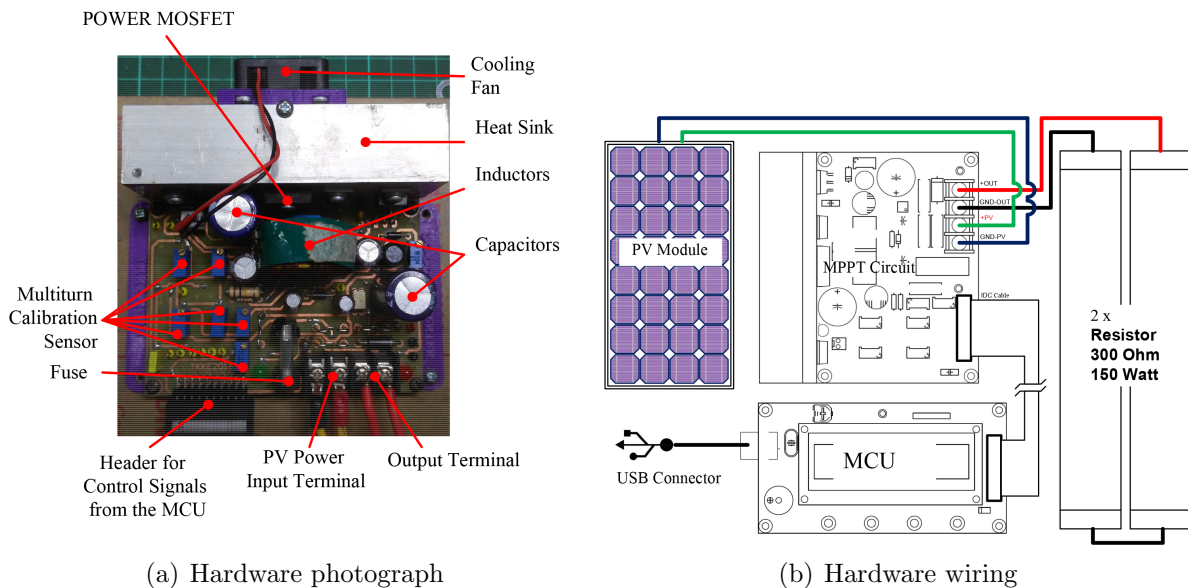


FIGURE 4. The photograph and wiring diagram of the electronic hardware

Figure 4(b) presents the hardware wiring diagram of the boards illustrated under simulated experimental situation. The output terminal of the MPPT circuit board is connected to a reconfigurable load cell (Resistor  $2 \times 300\Omega$ , 150 Watt). In the experiments, the load cell is set to 150, 300 and  $600\Omega$  to test the performance of the MPPT circuit. To set  $150\Omega$ , two resistors are configured in parallel connection. To set  $300\Omega$ , a single resistor is used, and to set  $600\Omega$ , two resistors are configured in series connection. The MCU board can also be connected to a PC through a USB connector. The data measurements from the voltage and current sensors are sent via this USB link. In the PC, a graphical user interface (GUI) is developed and installed for user interface.

In the MPPT board, a single-ended primary inductive converter (SEPIC) circuit is used to convert the DC input power from the PV panels into maximized DC output power. Two toroidal ferrite cores, having parameters  $1.5\text{mH}$ ,  $8.28\text{A}$ ,  $100\text{m}\Omega$ , are used to implement inductor elements in the circuit. The coupling capacitor,  $C_1$ , is set  $100\text{nF}$ , and the output capacitor,  $C_2$  is set  $1000\mu\text{F}$ , having  $50\text{V}$  rating. MOSFET type IRFP460 is used to implement the electronic switch. The PWM signal is generated using ATmega328P, an 8-bit microcontroller from Atmel, through a gate driver circuit using an optocoupler

(TLP250) and MOSFET driver (IR2117). Power from PV is used to supply the electronic devices using a step-down regulator LM2573.

The maximum power is obtained by finding the best duty cycle of a pulse-width modulated (PWM) signal applied to a MOSFET gate used in the SEPIC converter circuit. The MPPT algorithm embedded in the microcontroller will find this expected duty ratio using the proposed DWS algorithm. Two sensors, i.e., a voltage sensor and a current sensor, are used and sent to the microcontroller unit. The measured data from both sensors are calculated in the MPPT algorithm to obtain the PV power.

**3.3. The MPPT algorithm (embedded software).** The flow chart of the DWS MPPT algorithm is presented in Figure 5. The algorithm starts with three initial parameter values, i.e., **StartBit**, **EndBit** and **ScanWidth**. The **StartBit** is the first scan point of the scanning range (scan window). The **EndBit** is the last scan point, while the **ScanWidth** is the length of the scanning range. The **StartBit** and the **EndBit** points are always updated. The **ScanWidth** is set constant for all scanning processes. The **BitMax** is a temporary point, by which the temporary maximum power point value (**Pmax**) is obtained.

The **BalanceBit** is the step width value of the scanning process. For each iteration, the temporary **BitMax** is always set or located between the **StartBit** and the **EndBit**. Once scanning process gets started, the counting bit (**CntBit**) as the incremented scanning point, is set equal to the **StartBit**. Then, the scanning process starts looking for a maximum power point through the increment of the scanning point with the **BalanceBit** step width.

The proposed DWS algorithm works based on the following power measurement mechanism. The microcontroller generates a pulse with a certain duty ratio. When a higher power point is found larger than the previous power, a temporary maximum power value is stored as **Pmax**, as well as the point **BitMax**, that can generate the temporary power point **Pmax**. The algorithm will end, when the **BalanceBit** is zero, or the scanning process is finished, where in this case the maximum power point should have been found.

The MPPT algorithm is implemented on Atmega328 microcontroller from Atmel. The algorithm consumes 11,518 bytes memory, or 37% of total 30,720 byte available memory slots in the microcontroller. Moreover, the global variable uses 461 bytes (22%) of dynamic memory, leaving 1,587 bytes for local variables of maximum 2,048 bytes.

**4. Experimental Setup and Testing Results.** The electronic hardware has been tested under three different scenarios. Figure 6 presents the test setup of the three scenarios as well as the PV output power measurements for each scenario. The MPPT algorithm embedded on the microcontroller is then run to maximize the power transfer. As shown in the figure, the measured voltage and current sensor data are monitored and stored in the computer. A user interface is also designed to enable us to monitor online the power measurements. The specification of the used PV panel in the experiments is shown in Table 1. The panel is maximum rated power of 100 Watt. Its open-circuit is about 22.41V and its short-circuit current is about 6.2A.

The experiments are aimed at measuring the performance of the DWS algorithm. The testing is made using a single PV module under sun shine condition at 13:00 local time. Each of three partial scenarios is tested using 3 different resistance loads, i.e., 150, 300 and 600 Ohm. Partial shadows are made by covering some small surface areas of the PV module. Certainly, there are many other partial shadowing conditions that can be created. However, only three selected scenarios are tested in the experiments, which are explained in the following subsections.

Figure 6 shows three partial shading scenarios and their testing results show the PV power output measurements of each scenario. Figure 6(a) presents the partial shadow

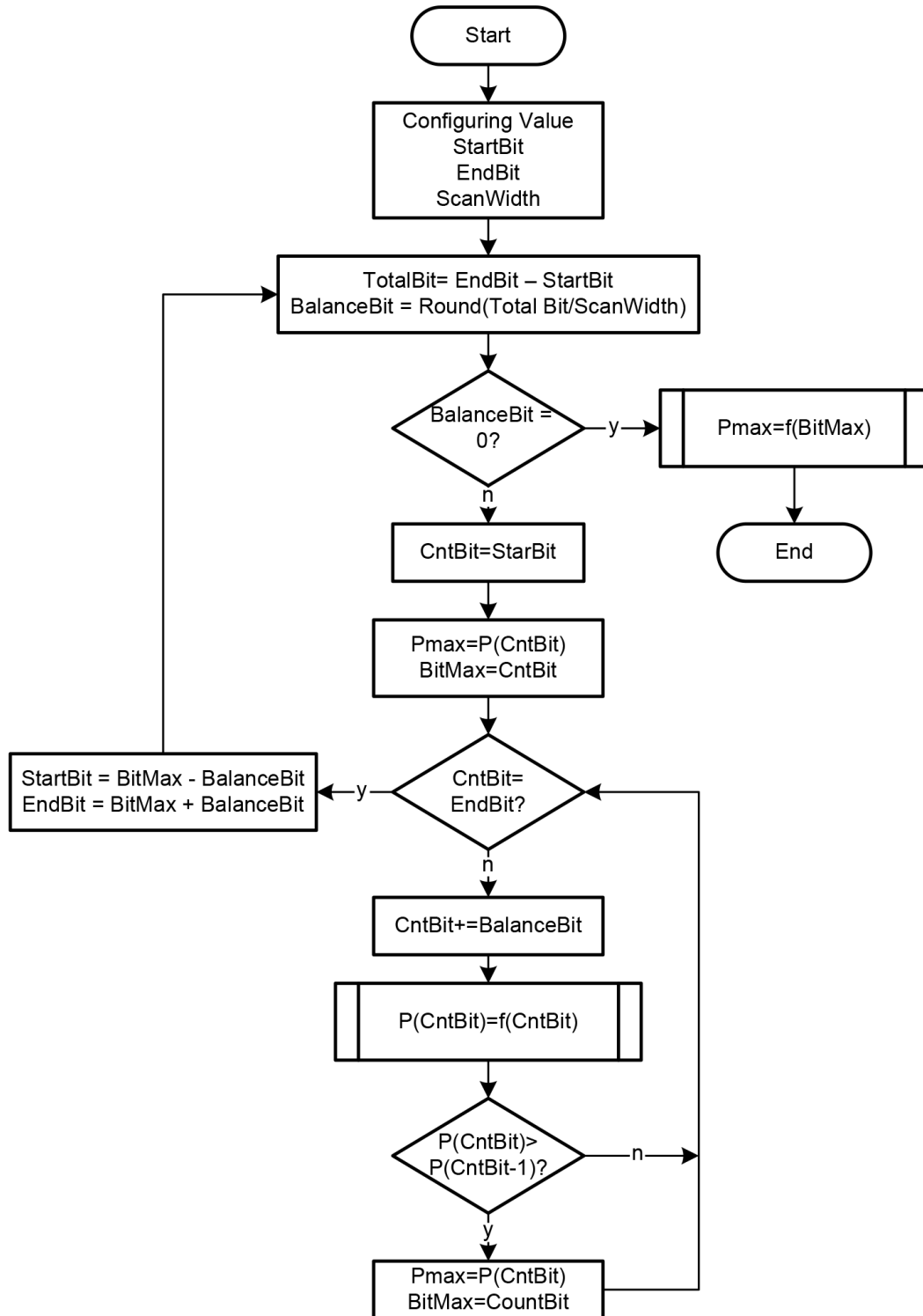
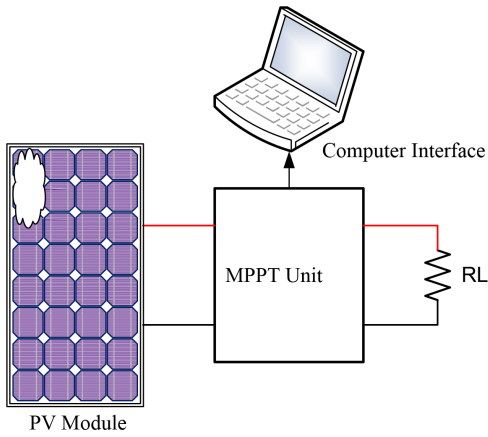
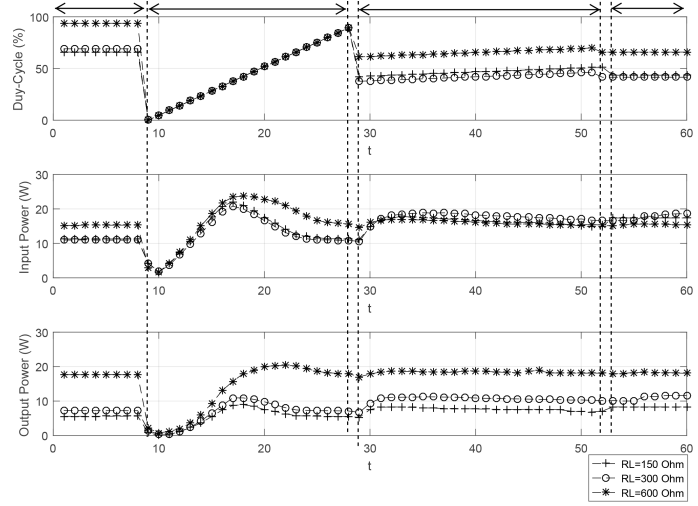


FIGURE 5. The flow chart of the decremented window-size scanning-based MPPT algorithm

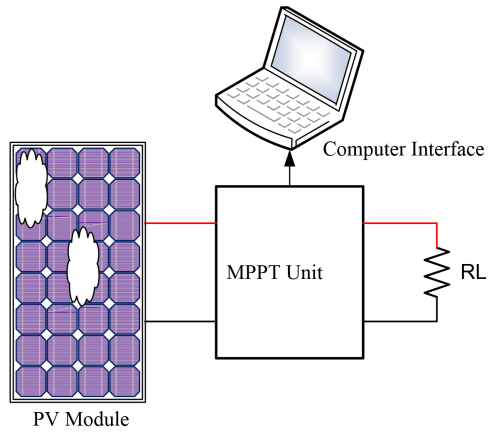
condition 1, where a covering material is applied on the upper-left side of the PV panel surface. The partial shadow condition 2 is presented in Figure 6(c), where the covering materials are respectively applied on the upper-left side and on the center of the PV panel surface. In the partial shadow condition 3 presented in Figure 6(e), three covering materials are applied on the upper-left side, on the center and on the bottom-left side, respectively, on the PV panel surface.



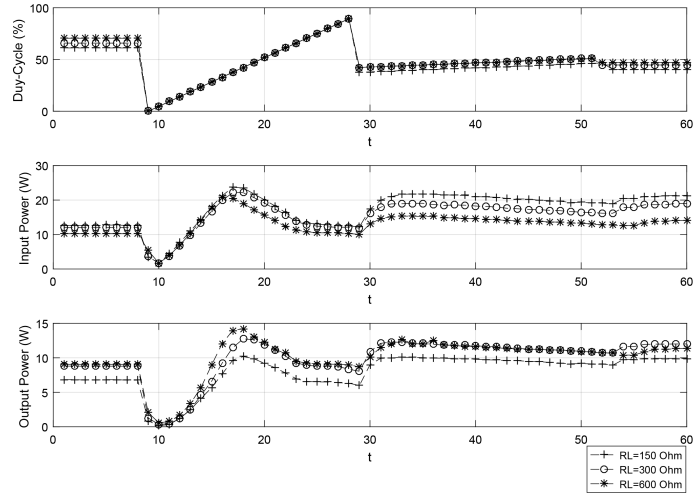
(a) Scenario 1 (Test setup)



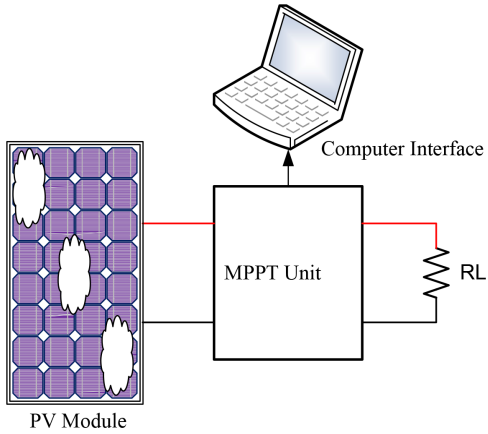
(b) Scenario 1 (Testing result)



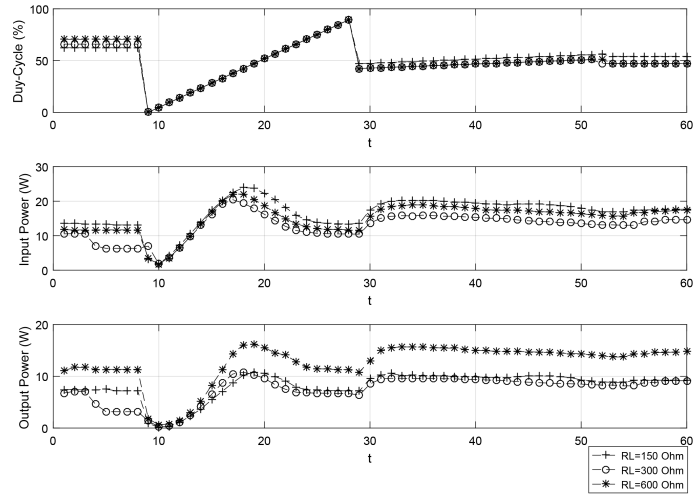
(c) Scenario 2 (Test setup)



(d) Scenario 2 (Testing result)



(e) Scenario 3 (Test setup)



(f) Scenario 3 (Testing result)

FIGURE 6. Partial shading scenarios and the testing results by measuring the PV power outputs

TABLE 1. The specification of the used PV panel

Rated maximum power	100w
$V_{OC}$ (Open-circuit voltage)	22.41
$V_{OP}$ ( $V_{mpp}$ )	17.9V
$I_{SC}$ (Short-circuit current)	6.2A
$I_{OP}$ ( $I_{mpp}$ )	5.59A
Output tolerance	+/-3%
Temperate coefficient of $I_{SC}$	+/-3%/°C
Temperate coefficient of $V_{OC}$	(0.10+/-0.01)%/°C
Temperate coefficient of power $V_{OC}$	-0.47%/°C
Temperature range	-40°C to +80°C
Frame	Heavy duty aluminum
Kind of glass and its thickness	Low iron, high transparency tempered glass of 3.2mm
SLA battery voltage	12V
Dimensions (L × W × H)mm	665 × 996 × 35mm (26.16 × 39.3 × 1.37 inch)
Weight	19.85lbs (9kg)

For the three scenarios, Figure 6(b), Figure 6(d) and Figure 6(f) show respectively three curves, i.e., the duty ratio, the input power of the MPPT circuit and the output power curve of the MPPT circuit for three different loads. The input power is related to the output power of the PV panel. It seems from the figure that MPPT algorithm tracks the power points by scanning the power using duty-ratio scanning. From all the aforementioned figures (all scenarios), it seems that in the first scanning step (the 9<sup>th</sup> until 28<sup>th</sup> scanning step), the significant differences of the input and output power curves are clear. In the first domain scanning windows, the MPPT module measures the power points using the perturbing PWM signals with 5% duty ratio until 90% duty ratio. In the second scanning step, the range of the duty ratios of the perturbing PWM signals becomes smaller. It then becomes smaller, in the third domain scanning window. The output powers show the same tendency for all scenarios. Those cases happen because the domain of searching area of the peak power points is reduced and finally the MPP is trapped or found.

From the three experiments with different partial shading scenarios, we can also see that the efficiency of the MPPT operation becomes better for higher load values. It means that the MPPT works more efficiently, when the PV system is not overloaded. Lower load value means that there are many loads connected in parallel, making the total load value lower. Table 2 gives the summary of the data measurements from the experiments.

In the experiments, the consumption of the microcontroller unit is measured. For instance, using 150Ω load under the partial shading condition 2, when the MPPT algorithm operates under partial shading scenario 2, the driver circuit consumes current about 0.02-0.24A, while the microcontroller consumes current about 0.05-0.34A. The consumed current by the microcontroller is measured at the voltage regulator terminal for the microcontroller. Unfortunately, as far as we try, we cannot find any references that report the power consumption of its electronic control unit and driver circuit. Hence, we cannot make a comparative study regarding this power aspect.

**5. Conclusions and Outlooks.** This paper has presented a simple method to trace maximum power points of the PC operation using scanning method. The window or frame size of the scanning domain is decremented in every step cycle. The decrease step

TABLE 2. Summary of the data measurements from the experiments

Scenario, Load in $\Omega$	$V_{IN}$ (Volt)	$V_{OUT}$ (Volt)	Duty (%)	$P_{IN}$ (Watt)	$P_{OUT}$ (Watt)	Eff. (%)
Scenario 1, 150	12.07	31.88	43.53	17.38	8.29	47.69
Scenario 1, 300	12.42	45.18	41.57	17.88	11.3	63.15
Scenario 1, 600	12.96	68.95	51.76	22.8	19.9	87.6
Scenario 2, 150	13.01	34.87	40.39	20.42	9.76	47.8
Scenario 2, 300	10.58	41.21	44.71	16.19	10.71	66.19
Scenario 2, 600	9.87	50.89	47.06	12.73	10.69	83.94
Scenario 3, 150	10.21	30.59	54.12	17.36	9.18	52.87
Scenario 3, 300	10.55	38.22	47.06	14.03	8.79	62.65
Scenario 3, 600	11.14	59.44	47.06	16.71	14.27	87.36

is intended to trap the maximum power operation points of the PV system under varying partial shading conditions. The DWS MPPT algorithm does not require prior information about the PV installation condition and can be implemented in a microcontroller with simple iterative programming algorithm. The MPPT is also simple to implement. It requires only 11,518 bytes memory, or about 37% of total 30,720 byte available memory slots in the used microcontroller.

The effectiveness of the proposed method has been tested in the real experiments under three different partial shading conditions with different load conditions. The average current consumption of the driver circuit for the different scenarios is about 20mA, and for the controller unit is about 30mA. Comparative study to other references regarding this aspect is not made, since as far as we try, we cannot find any references that report the power consumption of its electronic control unit and driver circuit.

Besides the advantageous feature of the MPPT method mentioned above, it leaves also any shortage. When the scanning is rescheduled due to the change of global MPP following climate change, the starting point of the scanning will start from the previously set initial point. In this condition, the maximum power delivery is interrupted for a while, although the global MPP will be finally found again. In the future, it is challenged to find the new initial starting point to avoid the aforementioned problem. Non-conventional and statistical methods can be proposed, combined with the existing technique, to find the best initial scanning point.

**Acknowledgement.** The authors gratefully acknowledge the Ministry of Finance, through Indonesia Endowment Fund for Education or *Lembaga Pengelola Dana Pendidikan (LPDP)* for funding our research project under the scheme of “Commercial-Intended Innovative Productive Research Grant” or *Riset Inovatif Produktif (RISPRO) Komersil* for the year 2019-2022 with Grant Contract Number PRJ-46/LPDP/2019.

## REFERENCES

- [1] F. Ronilaya, I. Siradjuddin, S. E. Wibowo and I. Ridzky, A new implementation of single phase Shimizu inverter for optimal power flow of solar PV system based on incremental conductance MPPT method, *ICIC Express Letters*, vol.12, no.7, pp.621-630, 2018.
- [2] M. Al-Dhaifallah, A. M. Nassef, H. Rezk and K. S. Nisar, Optimal parameter design of fractional order control based INC-MPPT for PV system, *Solar Energy*, vol.159, pp.650-664, 2018.
- [3] C.-T. Phan-Tan and N. Nguyen-Quang, A P&O MPPT method for photovoltaic applications based on binary-searching, *The IEEE International Conference on Sustainable Energy Technologies (IC-SET)*, 2016.

- [4] H. A. Sher and K. E. Addoweesh, A new sensorless hybrid MPPT algorithm based on fractional short-circuit current measurement and P&O MPPT, *IEEE Trans. Sustainable Energy*, vol.6, no.4, pp.1426-1434, 2015.
- [5] C. Lohmeier, J. Zeng, W. Qiao, L. Qu and J. Hudgins, A current-sensorless MPPT quasi-double-boost converter for PV systems, *Energy Conversion Congress and Exposition (ECCE)*, pp.1069-1075, 2011.
- [6] N. Bouarroudj, D. Boukhetala, V. Feliu-Batlle, F. Boudjema, B. Benlahbib and B. Batoun, Maximum power point tracker based on fuzzy adaptive radial basis function neural network for PV-system, *Energies*, vol.12, pp.1-19, 2019.
- [7] R. Arulmurugan and N. S. Vanitha, Intelligent fuzzy MPPT controller using analysis of DC to DC novel buck converter for photovoltaic energy system applications, *International Conf. on Pattern Recognition, Informatics and Mobile Engineering*, 2013.
- [8] A. Mohamed, A. Berzoy and O. Mohammed, Design and hardware implementation of FLMPPT control of PV systems based on GA and small-signal analysis, *The IEEE Power & Energy Society General Meeting*, 2017.
- [9] S. Farajdadian and S. H. Hosseini, Optimization of fuzzy-based MPPT controller via metaheuristic techniques for stand-alone PV systems, *International Journal of Hydrogen Energy*, vol.44, no.47, pp.25457-25472, 2019.
- [10] U. Yilmaz, O. Turksoy and A. Teke, Improved MPPT method to increase accuracy and speed in photovoltaic systems under variable atmospheric conditions, *International Journal of Electrical Power & Energy Systems*, vol.113, pp.634-651, 2019.
- [11] A. M. Farayola, A. N. Hasan and A. Ali, Efficient photovoltaic MPPT system using coarse Gaussian support vector machine and artificial neural network techniques, *International Journal of Innovative Computing, Information and Control*, vol.14, no.1, pp.323-339, 2018.
- [12] D. C. Huynh, T. M. Nguyen, M. W. Dunnigan and M. A. Mueller, Global MPPT of solar PV modules using a dynamic PSO algorithm under partial shading conditions, *The IEEE Conference on Clean Energy and Technology (CEAT)*, 2013.
- [13] S. Mohanty, B. Subudhi and P. K. Ray, A new MPPT design using grey wolf optimization technique for photovoltaic system under partial shading conditions, *IEEE Trans. Sustainable Energy*, vol.7, no.1, pp.181-188, 2016.
- [14] H. Chaieb and A. Sakly, A novel MPPT method for photovoltaic application under partial shaded conditions, *Solar Energy*, vol.159, pp.291-299, 2018.
- [15] A. Harrag and S. Messalti, IC-based variable step size neuro-fuzzy MPPT improving PV system performances, *Energy Procedia*, vol.157, pp.362-374, 2019.
- [16] Y. Sugimoto, The solar cells and the battery charger system using the fast and precise analog maximum power point tracking circuits, *IEEE Computer Society Annual Symposium on VLSI*, 2015.
- [17] C.-L. Shen, Y.-S. Shen and C.-T. Tsai, Design and implementation of an analog circuit with minimum component count for double-linear-approximation MPPT, *ICIC Express Letters, Part B: Applications*, vol.7, no.11, pp.2443-2449, 2016.
- [18] G. Chen, X. Dong, S. Dai, H. Li and K. Peng, Application of partitioned self-adaption variable step size MPPT algorithm in PV system, *ICIC Express Letters, Part B: Applications*, vol.9, no.6, pp.575-583, 2018.
- [19] M. Morales-Caporal, J. Rangel-Magdaleno and R. Morales-Caporal, Digital simulation of a predictive current control for photovoltaic system based on the MPPT strategy, *The 13th International Conference on Power Electronics (CIEP)*, pp.295-299, 2016.
- [20] B. Hossam and K. Itako, Real time hotspot detection using scan-method adopted with P&O MPPT for PV generation system, *The 2nd Annual Southern Power Electronics Conference (SPEC)*, pp.1-5, 2016.
- [21] K. Chen, S. Tian, Y. Cheng and L. Bai, An improved MPPT controller for photovoltaic system under partial shading condition, *IEEE Trans. Sustainable Energy*, vol.5, no.3, pp.978-985, 2014.